Fracture Mechanics Analysis of Composites with Ply-Drops - Measurement of Delamination Fatigue Crack Growth Rate

Goutianos, Stergios; Sørensen, Bent F.

Publication date:
2018

Document Version
Peer reviewed version

FRACTURE MECHANICS ANALYSIS OF COMPOSITES WITH PLY-DROPS - MEASUREMENT OF DELAMINATION FATIGUE CRACK GROWTH RATE

Stergios Goutianos and Bent F. Sørensen

Section of Composites and Materials Mechanics, Department of Wind Energy, Technical University of Denmark, Roskilde, Denmark
Email: gout@dtu.dk, Web Page: http://www.vindenergi.dtu.dk
Email: bsqr@dtu.dk, Web Page: http://www.vindenergi.dtu.dk

Keywords: Tunneling crack, delamination, cohesive law, fatigue crack growth rate

Abstract
Ply-drops must be taken into account in the design of composite structures due to the initiation and propagation of delaminations at ply-drop locations. This damage mode is experimentally investigated in tension-tension fatigue and the fatigue delamination growth rate is measured for two (external and internal) ply-drop geometries. It is found that the fatigue delaminations grow at a constant rate. Fracture mechanics, using the finite element method, is used to analyse the ply-drops. The influence of material and geometric parameters on the fracture energy release rate is investigated.

1. Introduction

The overall external geometrical shape of many lightweight composite structures (e.g. aerofoil shape for a wind turbine rotor blade) is specified by aerodynamic considerations. An additional requirement is to minimize the weight of the structure but without significant drop in stiffness and strength [1]. These requirements are achieved by thickness variation of the load-carrying laminates by "terminating" or dropping off plies (ply-drops) at the locations where the geometry changes. Ply-drops result in geometrical and material discontinuities that are potential sources for delamination initiations and propagation [2] resulting in a severe reduction of the load carrying capability of the composite structures.

Several studies investigated the initiation and propagation of delaminations in tapered composites [3-6]. The analytical and numerical techniques use stress-based criteria and/or fracture mechanics based criteria [1,2]. Despite the large amount of research devoted to predict the effect of ply-drops on the structural strength, challenges still exist a) in accurate strength (static and fatigue) predictions and b) in designing more damage tolerant tapered composites by investigating the parameters that influence the onset and growth of the delaminations.

The present study is an ongoing effort towards the development of a robust, fracture mechanics based, methodology to predict the initiation and propagation of delaminations initiating at ply-drops. Such a methodology can also be used to create tapered composites that possess high damage tolerance. This can lead to damage tolerance design of composite structures (e.g. a wind turbine rotor blade) where damage is accepted as long it can be detected and its growth will be stable and can be accurately predicted [7]. To identify the failure mechanism simplified composite specimens with ply-drops are tested in cyclic loading and analysed numerically using fracture mechanics methods. Both external ply-drops (the dropped plies are on the surface of the laminate) and internal ply-drops are examined.

2. Experimental Details

2.1. Materials, Stacking sequence and dimensions of the ply-drop specimens

Unidirectional glass fibre/epoxy specimens with ply-drops were manufactured by vacuum infusion and had a fibre volume fraction of 0.5. The nearly unidirectional glass fibre fabric was obtained from Saertex. The fabric areal weight was 1134 g/m^2 with the areal weight of the 90^o fibres (backing fibres) being equal to 54 g/m^2 and polyester fibres as sewing threads. The epoxy matrix material, Araldite® LY 1568, and the hardener, Aradur® 3489 CH, were obtained from Huntsman. The curing cycle of the ply-drop specimens was 19 hrs at 40 ^{o}C followed by 5 hrs at 75 ^{o}C.

Two different types of ply-drops specimens were used as shown in Fig. 1. For the specimen type A, the dropped plies are on the surface (external ply-drops), whereas for specimen type B the ply-drops are internal. Each specimen had four plydrops at uneven positions along the specimen length. Each ply drop was formed by a single fabric layer with a thickness of 1 mm after consolidation. The composite beam consisted of ten layers. All layers were placed in vacuum infusion table with the backing fibres on the bottom side. For the specimen type A (see Fig. 1b), a perforated slip foil of length equal to 20 mm and 20 μm in thickness was placed between the composite beam and the first ply-drop. The slip foil was used to initiate the delamination crack. The specimen type B includes an additional continuous biaxial (±45^o) layer placed on top of the ply drops as shown in Fig. 1b. For the specimens type B, a starting crack (slip foil) was not used. For all specimens ±45^o glass/fibre epoxy tabs were glued on one side of the specimens (see Fig. 1a). The tabs were added to create specimens with equal thickness at the ends that could be mounted on a tensile testing machine.

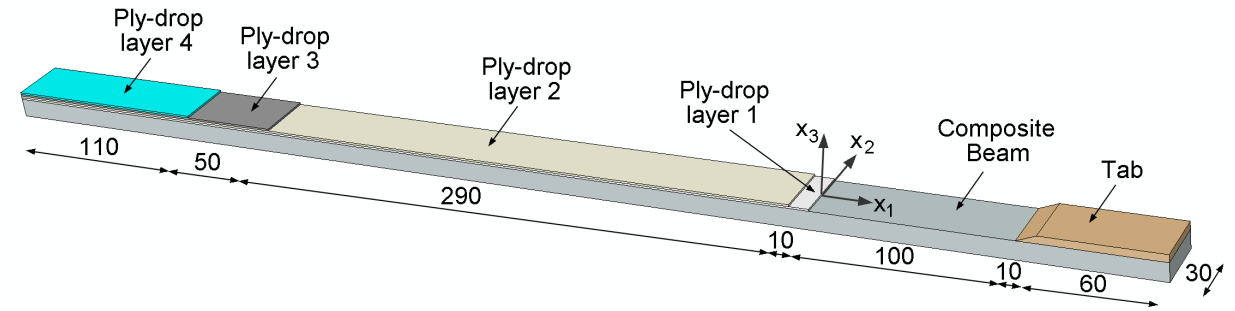

a) Specimen dimensions and position of the ply-drops

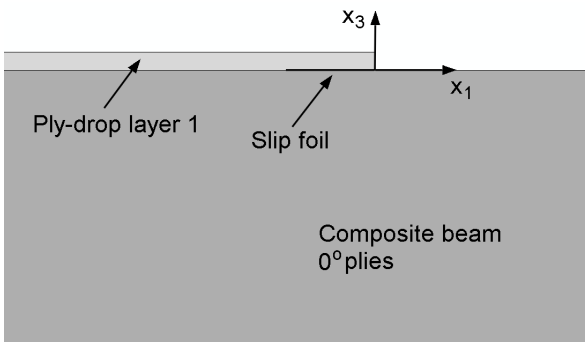

b) Type A ply-drop specimen type A (external ply-drops)

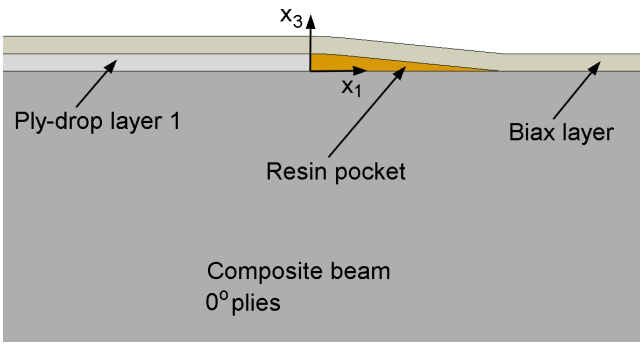

c) Type B ply-drop specimen type B (internal ply-drops)

Figure 1. Dimensions of the plydrop specimens and details of the ply-drop design for the two different specimen types (all dimensions in mm).

2.2. Loading arrangement and procedure

Four ply-drop specimens were subjected to a monotonically increasing tensile loading in a hydraulic testing machine to measure the stiffness of the specimens and the bending ratio (due to the asymmetry of the ply-drop specimen geometry). The bending ratio was measured by two strain gauges glued on the opposite faces in the thin section of the ply-drop specimens (x_1=60 mm).

The cyclic tests were performed between fixed stress values at a frequency of 3 Hz. The R-ratio was equal to 0.1. Photographs of the specimen were obtained at a predefined number of cycles in order to measure the fatigue delamination crack length. Several crack growth measurements at different maximum applied load could be obtained from a single specimen when the delamination was in the region with two ply-drop layers (see Fig. 1a). Following testing, several specimens were examined by SEM.

3. Experimental Results

Fig. 2 shows a series of photographs taken from a ply-drop specimen of type A tested under cyclic loading. The crack front is nearly constant across the specimen width (x_2 direction). The crack extension with the number of cycles can be easily seen and measured. From such measurements, the fatigue crack growth rate can be derived as shown in Fig. 3. It should be mentioned that in the present study, the reported fatigue crack growth rates are measured in the region ply-drop layer 2 (see Fig. 1a) were the height of the ply-drop specimens is constant. Fig. 3 shows that the crack growth rate is constant and increases with increasing the maximum applied stress.

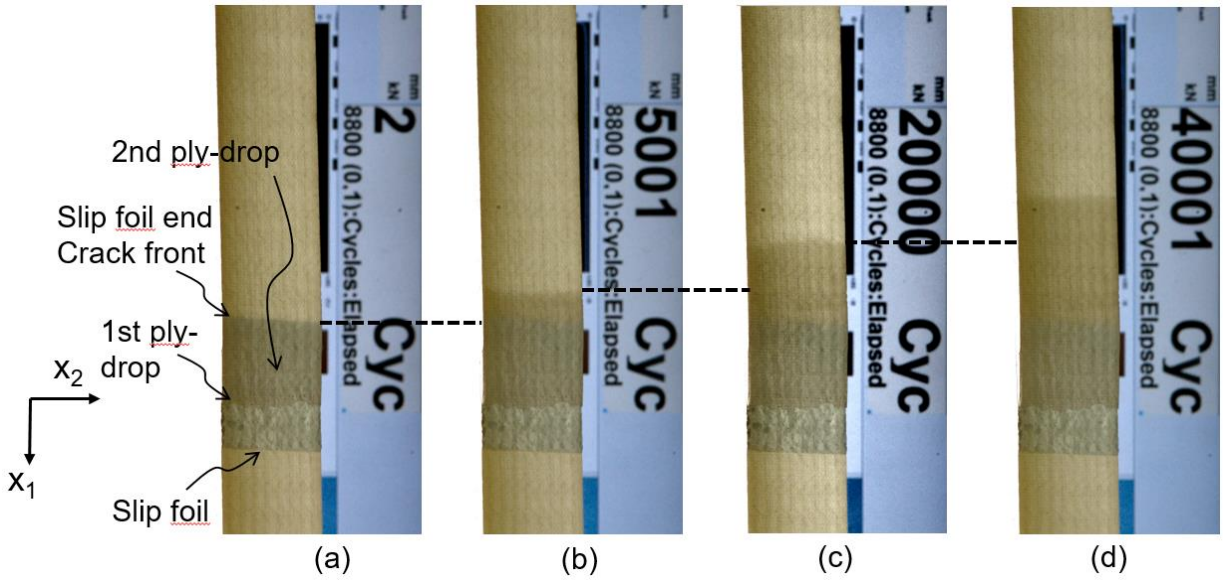

Figure 2. Fatigue delamination crack growth for a ply-drop specimen of type A (see Fig. 1b): a) 2 cycles, b) 5000 cycles, c) 20000 cycles and d) 40000 cycles. σ_{max}=148 MPa.

The fatigue crack initiation and growth for a ply-drop specimen of type B is shown in Fig. 4. Since in this specimen there is no a starting crack (slip foil), crack initiation occurs (after approximately 3000 cycles) as tunneling cracks in plydrops 1 and 2. Then, the fatigue crack grows in the region of ply-drop 2. Crack growth towards the resin rich area (in the positive x_1 direction, opposite the main delamination crack) is minimum as shown in Fig. 4c. With increasing number of cycles, the crack continues to grow in the ply-drop 2 region but also it grows in the opposite direction towards the thin section (see Fig. 1a).

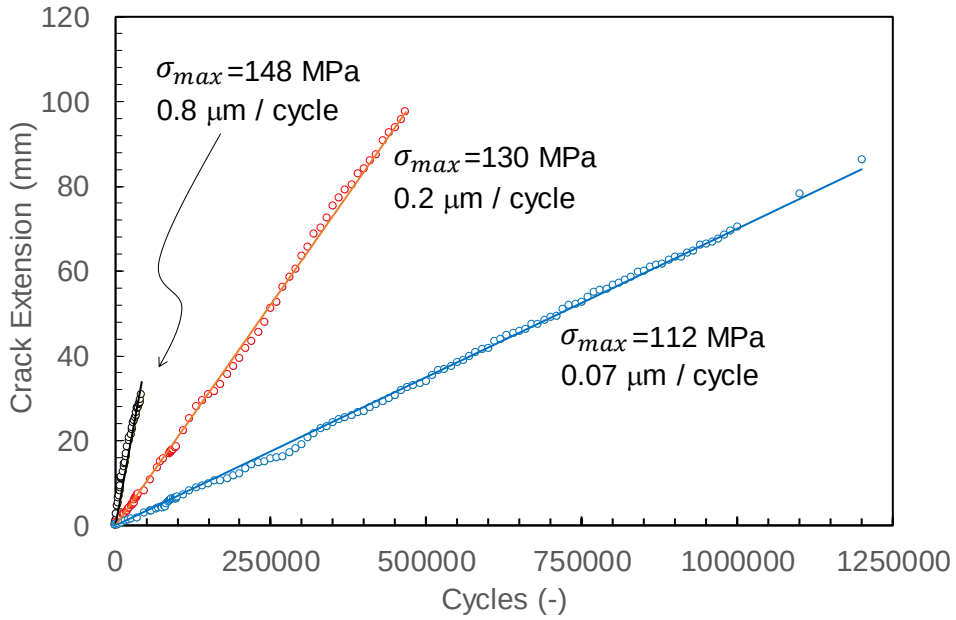

Figure 3. Measured fatigue delamination crack growth for a ply-drop specimen of type A (see Fig. 1c) as a function of the number of cycles for three different maximum applied stress levels.

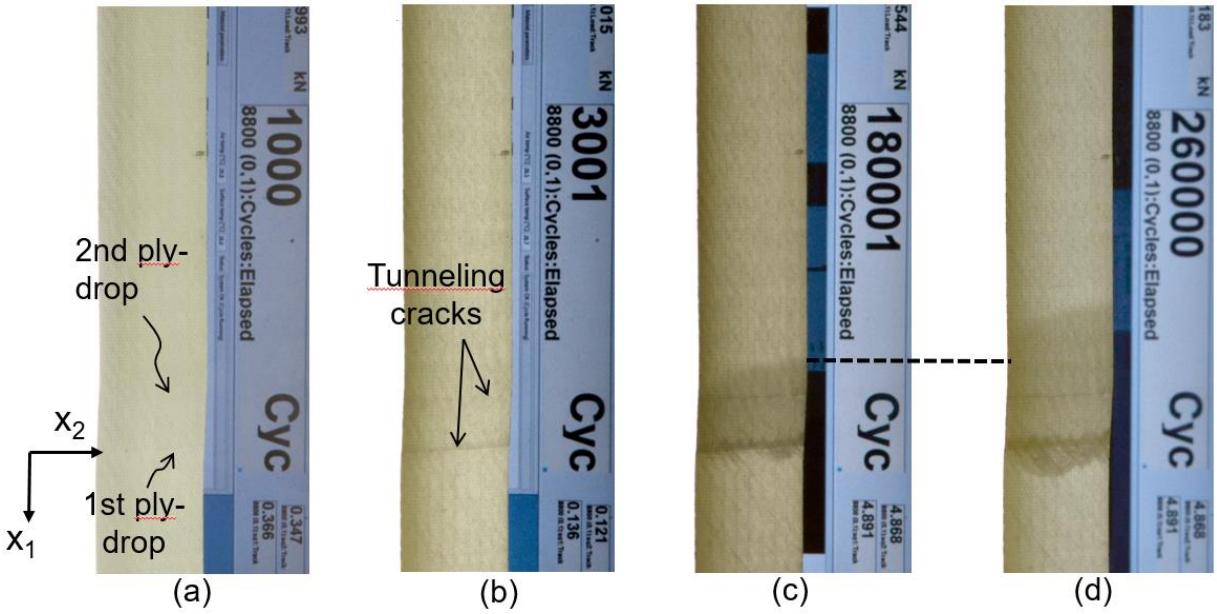

Figure 4. Fatigue delamination crack growth for a ply-drop specimen of type B (see Fig. 1c): a) 1000 cycles, b) 3001 cycles, c) 180001 cycles and d) 260000 cycles. σ_{max}=125 MPa.

The fatigue delamination crack growth rates, for both types of ply-drop specimens, is shown in Fig. 5 as a function of the maximum applied stress. It should be mentioned that the maximum applied stress is the average stress in the thin section of the specimens. The fatigue crack growth rate is slower for the ply-drop specimen of type B except for high applied stresses. More experiments are required to reduce the level of uncertainty.

The scanning electron microscopy photographs of Fig. 6 show the failure mechanisms for the ply-drop specimens of type B. First, a (tunneling) crack occurs between the first ply-drop and the resin rich area (see also Fig. 4b). Then, with increasing number of cycles a delamination crack initiates and propagates at the interface between the first ply-drop layer and the composite beam. The presence of

the backing fibres appears to be a weak interface and the crack path does not change during the entire fatigue tests, which were stopped when the crack front reaches the third ply-drop (see Fig. 1a). A second delamination crack initiates on the interface between the first ply drop layer and the biax layer. The path of this crack strongly depends on the local fibre bundle spatial location of the biax layer. In most cases it was observed that this crack run for a short distance towards ply-drop 2 and then arrested by reaching the free surface of the specimen. In some cases, this crack also propagated towards the thin section of the specimens, along the resin rich area / biax layer interface as seen in Fig. 6b. Crack propagation in this direction usually arrested when the crack front reached the thin section.

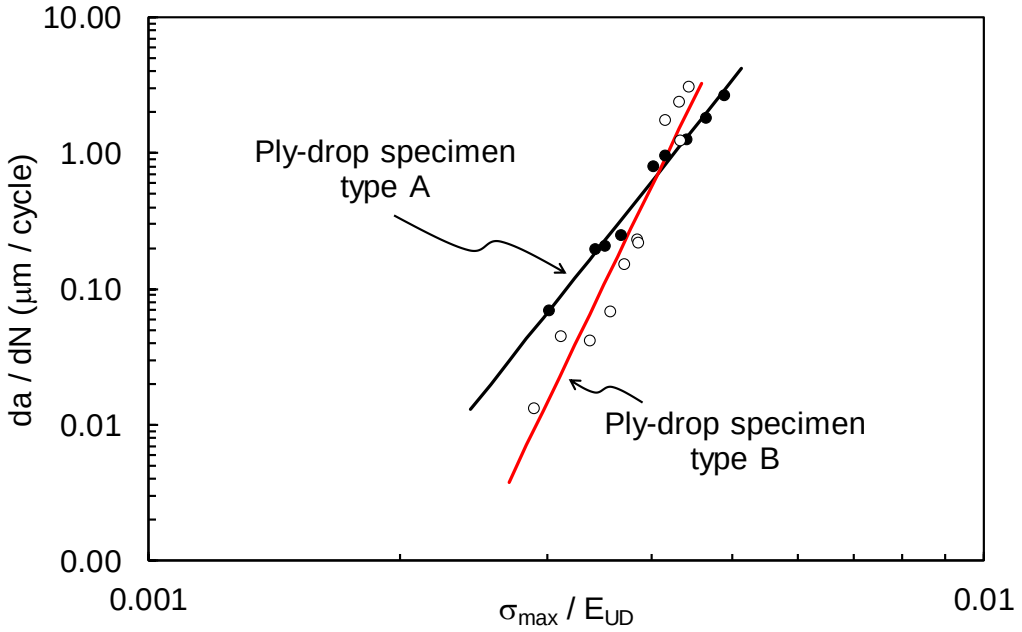

Figure 5. Fatigue delamination crack growth rates for the ply-drop specimens of type A (Fig. 1b) and B (Fig. 1c). The maximum applied stress is the average stress in the thin section.

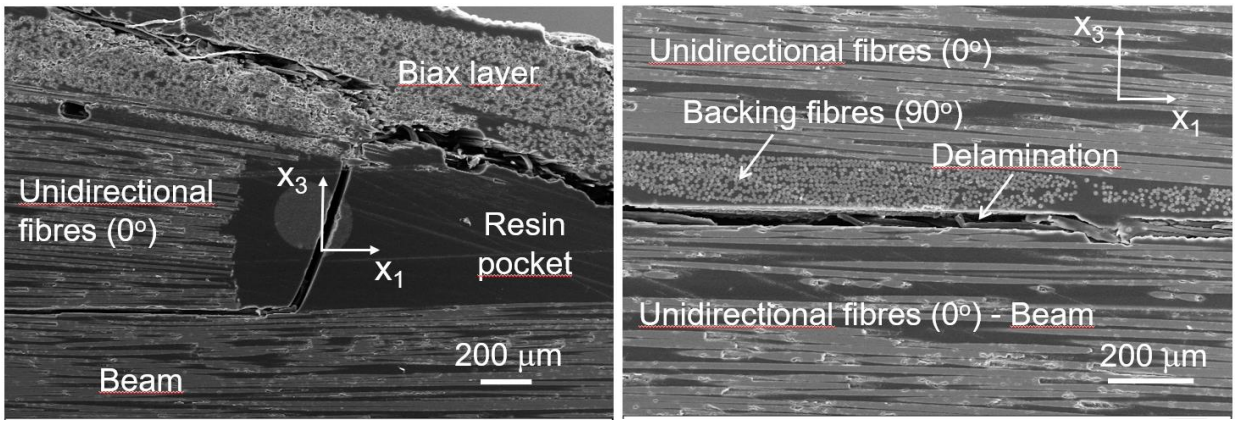

(a) (b)

Figure 6. ESEM photographs of a ply-drop specimen of type B (Fig. 1c) after fatigue tests: a) View of the failure mechanisms at the first ply-drop, b) detailed view of the crack path between the ply-drop layer 1 and the composite beam.

4. Finite Element Analysis of the Tunneling Crack

A parametric two-dimensional plane-strain finite element analysis was performed to investigate the

steady-state energy release rate of the tunneling cracks (Figs 4b and 6) for the ply-drop specimens of type B. The model represents a geometry similar to Fig. 1a but it contains only one ply-drop as shown in Fig. 7. For simplicity all materials are assumed to have a linear isotropic elastic behaviour. For each case, two models were solved [8]: a model to extract the stresses at interface between the ply-drop layer and the resin rich area (Fig. 7a) and a model, with a physical crack, to extract the crack opening displacement differences between the ply-drop layer and the resin rich area (Fig. 7b). The steady-state energy release rate is then given by [8]:

$$G_{ss} = \frac{1}{2h}\left\{\int_0^h \sigma_n\,(x_3)\delta_n(x_3)dx_3 + \int_0^h \sigma_t\,(x_3)\delta_t(x_3)dx_3\right\} \quad (1)$$

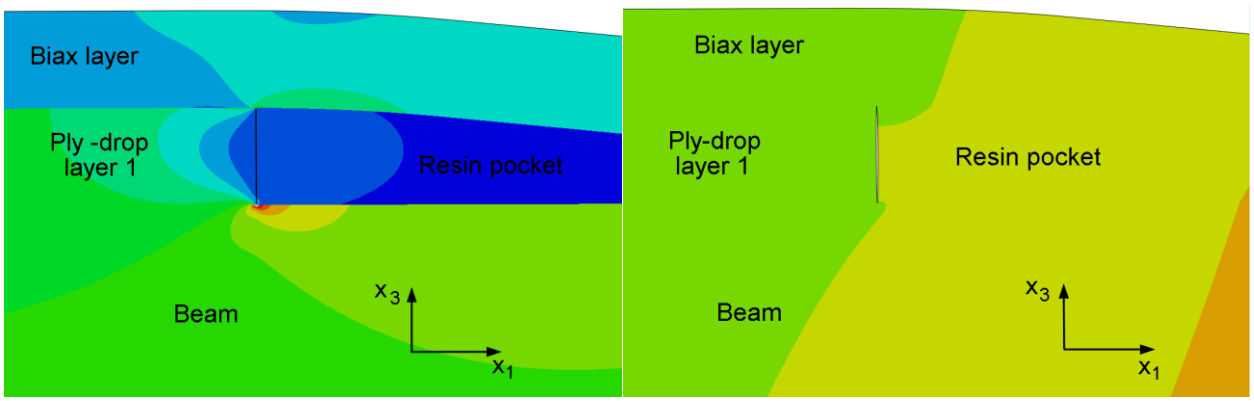

(a) (b)

Figure 7. Plane strain finite element models to analyse the tunneling crack at the ply-drop layer / resin rich area interface: a) model to extract stresses at the interface (stress σ_{11} contour), b) mode to extract crack openings (displacement u_1 contour).

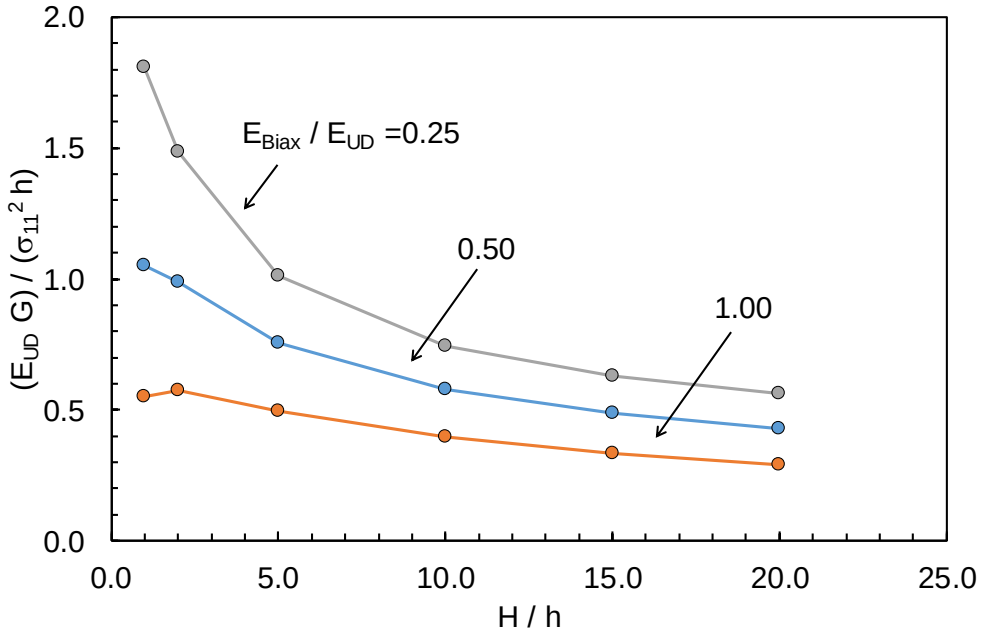

Figure 8. Effect of the beam height, H, and biax layer Young's modulus, E_{Biax}, on the steady-state energy release rate of the tunneling crack. The Young's modulus of the ply-drop layer and the beam is E_{UD} and the height of the ply-drop layer is h.

Fig. 8 shows the calculated steady-state energy release rate as a function of the ratio *h/H* for biax layers with different Young's modulus relative to the unidirectional layers. It is shown that an increase of the Young's modulus of the biax layer or an increase of the composite beam height result in a decrease of the steady-state energy release rate.

5. Finite Element Analysis of the Delamination crack

Once the tunneling crack is fully developed, the delamination initiates and propagates along the specimen length between the ply-drop layers and the composite beam (see Fig. 4). The analysis of the delamination is presented for the specimens of type A (external ply-drops). Fig. 9 shows the finite element mesh used for modelling a single ply-drop. A crack length of different length is introduced between the ply-drop layer and the beam. Then a prescribed displacement is applied to the thin section of the model and the mode I and mode II stress intensity factors are computed. The results are given in Fig. 10 for different *h/H* ratios. It can be seen that once the crack length is larger than the height of the ply-drop layer, both the mode I and mode II stress intensity factors attain a constant value. Since the mode I stress intensity factor is slightly lower than the magnitude of the mode II stress intensity factor, the delamination propagation for this type of specimens is a mixed mode problem. The computed mode mixity is 62º for *h/H*=1, 55º for *h/H*=2 and 52º for *h/H*>5.

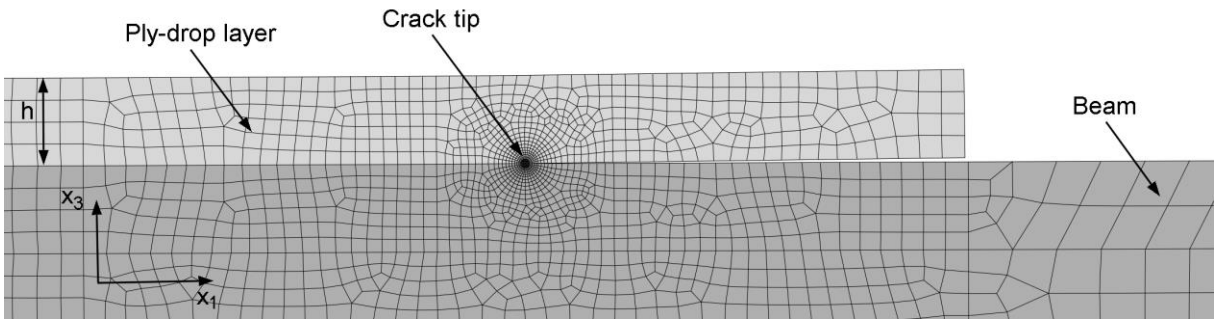

Figure 9. Plane strain finite element model to compute the mode I and mode II stress intensity factors for a deamination of a fixed length in ply-drop specimens of type A. (the deformed mesh is scaled to illustrate the crack opening).

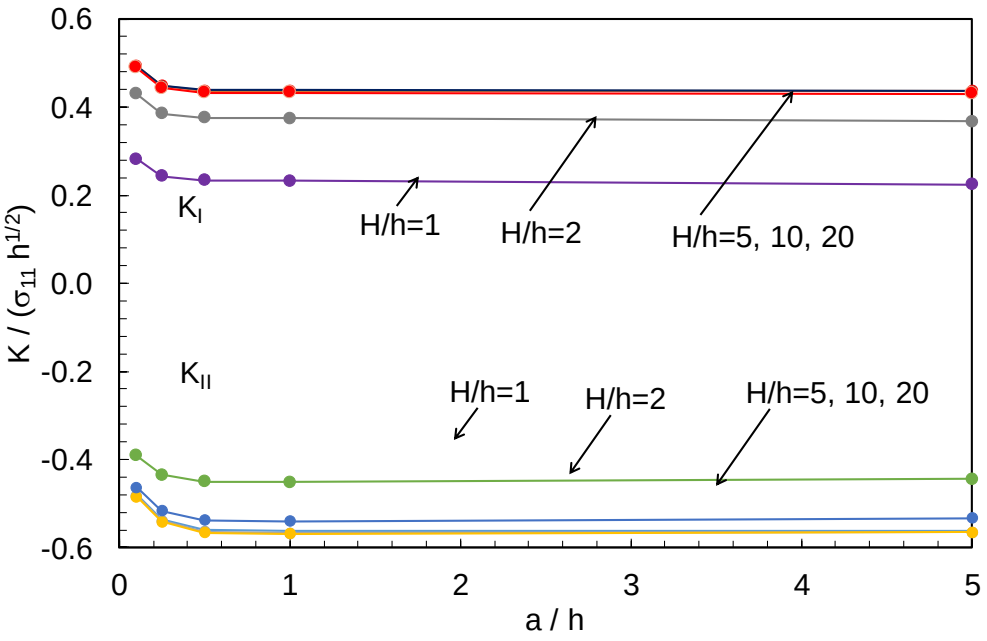

Figure 10. Mode I and mode II stress intensity factors as a function of the delamination crack length for the ply-drop specimen of type A (Fig. 1b) for different beam to ply-drop layer thickness ratios.

A similar analysis was performed for the specimens of type B with one crack introduced between the ply-drop layer and the beam and a second crack of equal length between the ply-drop and biax layers. Similar to Fig. 10, once the lengths of the cracks are larger than *h*, the stress intensity factors of both cracks attain a constant value. However, the mode mixity for the crack between the ply-drop layer and the beam is ≈80° and 90° for the crack between the ply-drop and biax layers, respectively. Thus, a significant difference in the mode mixity exists between external and internal ply-drops.

Moreover, the magnitude of stress intensity factor for the crack between the ply-drop layer and beam is larger than the magnitude of stress intensity factor between the ply-drop and biax layers. This implies that the crack growth rate will be largest for the crack between the ply-drop layer and the beam.

6. Summary and Conclusions

The tension-tension delamination fatigue crack initiation and growth rate initiated at ply-drops was experimentally investigated. Two different specimen types were used. One with external ply-drops and one with internal ply-drops. It was shown that the delamination growth rate attains a constant value once the delamination/crack length is larger than the ply-drop layer height.
Fracture mechanics was used to analyse the failure mechanisms observed in the fatigue experiments: a) tunneling crack at the interface of the ply-drop layer and the resin rich area for the specimen with internal ply-drops, and b) delamination at the ply-drop interface for specimens with external and internal ply-drops.

Acknowledgments
This work has received funding from the European Unions Horizon 2020 Research and Innovation Programme under Grant Agreement No 761072 (DACOMAT). Leonardo Di Crescenzo is acknowledged for manufacturing the test specimens and Hans Christian Jensen for technical assistance in the mechanical testing.

References

[1] K.W. Gan, G. Allegri and S. R. Hallett. A simplified layered beam approach for predicting ply drop delamination in thick composite laminates. *Materials and Design*, 108:570–580, 2016.

[2] K. He, S.V. Hoa, R. Ganesan. The study of tapered laminated composite structures: a review. *Composites Science and Technology* 60:2643-2657. 2000.

[3] M.R. Wisnom, M.I. Jones and W. Cui. Failure of tapered composites under static and fatigue tension loading. *AIAA Journal*. 33:911-918, 1995.

[4] G.B. Murri, T.K. O'Brien and C.Q. Rousseau. Fatigue life methodology for tapered composite flexbeam laminates. *Journal of the American Helicopter Society*. 43:146-155, 1998.

[5] O.T. Thomsen, W. Rits and D.C.G. Eaton. Ply drop-off effects in CFRP/honeycomb sandwich panels – theory. *Composites Science and Technology*. 56:407-422, 1996

[6] O.T. Thomsen and F. Mortensen. A simple approach for the analysis of embedded ply drops in composite and sandwich laminates. *Composites Science and Technology*. 59:1213-1226, 1999

[7] M. McGugan, M. Pereira, B. F. Sørensen, H. Toftegaard and K. Branner. Damage tolerance and structural monitoring for wind turbine blades. *Philosophical Transactions A*. 373:20140077, 2015.

[8] S. Ho and Z. Suo. Tunneling cracks in constrained layers. *Journal of Applied Mechanics-Transactions of the ASME*. 60:890-894, 1993.